Society of Medical Education & Research

2024, Volume 4, Issue 2, Page No: 127-140
ISSN: 3108-4826

Journal of Medical Sciences and Interdisciplinary Research

GC–MS and NMR-Based Investigation of Atriplex leucoclada with In Vitro and In Silico Assessment of COX Inhibition

Jonas Frederik Nielsen[1]*, Thomas Emil Rasmussen[1]

[1]Department of Management, Aarhus BSS, Aarhus University, Aarhus, Denmark.

***E-mail** ✉ j.nielsen.au@outlook.com

Abstract

Plants have traditionally served as a rich reservoir of medicinal compounds, yet numerous species remain underexplored in terms of their chemical composition and pharmacological properties. While many Atriplex species have undergone extensive examination, A. leucoclada, a halophyte endemic to the deserts of Saudi Arabia, has not been thoroughly assessed for its secondary metabolites or therapeutic capabilities. The present research evaluated the chemical profile and anti-inflammatory effects of A. leucoclada. The dried aerial portions of the plant were first treated with n-hexane to remove lipids, after which the residue was extracted using 80% methanol. The n-hexane fraction (ATH) underwent GC–MS analysis, whereas the methanol fraction (ATD) was fractionated through various chromatographic techniques to yield primary natural products. Structural determination of the isolated compounds relied on spectroscopic approaches, incorporating sophisticated NMR methods. The in vitro inhibitory effects of both fractions on COX-1 and COX-2 were assessed. In silico docking of the characterized molecules into the binding pockets of COX-1 (PDB: 6Y3C) and COX-2 (PDB: 5IKV) was performed.

Chemical analysis of the ATD fraction resulted in the isolation and characterization of nine compounds. Notably, with the exception of 20-hydroxy ecdysone (1), all were documented for the first time in A. leucoclada, and luteolin (6) as well as pallidol (8) represent novel findings within the Atriplex genus. Both ATD and ATH demonstrated dose-dependent inhibition of COX-1 and COX-2, with IC50 values of 41.22 and 14.40 µg/ml for ATD, and 16.74 and 5.96 µg/ml for ATH, respectively. Selectivity ratios were calculated as 2.86 for ATD and 2.80 for ATH, compared to 2.56 for Ibuprofen, suggesting preferable inhibition of COX-2. Docking simulations corroborated the experimental data, showing binding energies from -9 to -6.4 kcal/mol and -8.5 to -6.6 kcal/mol for the isolated compounds against COX-1 and COX-2, respectively; similarly, compounds detected via GC–MS exhibited values from -8.9 to -5.5 kcal/mol and -8.3 to -5.1 kcal/mol, versus Ibuprofen's -6.9 and -7.5 kcal/mol. Most compounds displayed strong affinities, with interaction modes varying according to structural features. These findings position A. leucoclada as a promising reservoir of anti-inflammatory natural products.

Keywords: A. leucoclada, NMR, GC–MS, COX, Anti-inflammatory, Molecular docking simulation

Introduction

Inflammation represents a protective response activated by infection, damage to tissues, physical trauma, or disruption of homeostasis. It involves the release of prostaglandins derived from arachidonic acid through the action of cyclooxygenase (COX) enzymes [1, 2]. These enzymes catalyze the biosynthesis of key mediators known as prostanoids, encompassing prostaglandins, prostacyclin, and thromboxane. Two main isoforms exist: COX-1, which is constitutively active in various tissues, particularly gastric mucosa and kidneys, and COX-2, which is inducible and upregulated during inflammatory processes. Targeting COX pharmacologically can alleviate inflammatory symptoms and associated pain [3].

Anti-inflammatory therapeutics encompass corticosteroids and nonsteroidal agents. Corticosteroids, however, are associated with severe adverse reactions,

Access this article online https://smerpub.com/

Received: 04 August 2025; **Accepted:** 21 November 2025

How to cite this article: Nielsen JF, Rasmussen TE. GC–MS and NMR-Based Investigation of Atriplex leucoclada with In Vitro and In Silico Assessment of COX Inhibition. J Med Sci Interdiscip Res. 2024;4(2):127-40. https://doi.org/10.51847/UNLmPnU9kl

including osteoporosis, immunosuppression, muscle weakness, cardiovascular complications, ocular issues, metabolic disturbances, psychological effects, and gastrointestinal or skin problems, restricting their long-term application relative to nonsteroidal options [4]. Nonsteroidal agents also carry risks such as respiratory issues, kidney impairment, thrombotic events, and gastric hemorrhage [5]. To address these limitations, investigations into botanical sources and isolated phytocompounds have intensified, aiming to discover safer anti-inflammatory alternatives [6–8] or adjuncts to conventional treatments [9].

The genus Atriplex (Amaranthaceae) comprises halophytic herbs with approximately 260 species distributed globally, predominantly in dry and semidry zones across Europe, Asia, Africa, Australia, and North America [10, 11]. Certain species exhibit substantial nutritional profiles, including high protein levels suitable for grain substitution, as seen with A. hortensis seeds [12]. Chemical studies on various Atriplex taxa have identified diverse classes of metabolites, such as phenolics [13, 14], triterpenes and sterols [15], phytoecdysteroids [16, 17], and saponins [13, 15, 18, 19]. Biologically, several species demonstrate anti-inflammatory [20], antioxidant, anticholinesterase [13], antidiabetic [21], antimicrobial [22], liver-protective [23], immunomodulatory [14], analgesic, antipyretic, and cytotoxic properties [24, 25].

Atriplex leucoclada Boiss. (common names: cut-leaf saltbush or orach; Arabic: Ragal, رغل) is a dwarf perennial shrub prevalent in Saudi Arabian arid landscapes. It holds ecological value in saline environments and adapts through specialized mechanisms [13, 26]. Literature review indicates limited prior work on its chemistry or bioactivity, with only one report describing five triterpenoid saponins and their molluscicidal effects [27]. Therefore, this investigation aimed to expand knowledge on the secondary metabolites and anti-inflammatory properties of A. leucoclada.

Materials and Methods

General experimental procedures

Nuclear magnetic resonance spectra were recorded on a Bruker Avance III 400 MHz instrument equipped with a BBFO Smart Probe and a Bruker 400 MHz AEON Nitrogen-Free Magnet (Bruker AG, Switzerland), operating at 400 MHz for ^{1}H and 100 MHz for ^{13}C. Spectral data were processed with Topspin 3.1 software (Bruker AG, Fallanden, Switzerland). Standard Bruker pulse sequences were employed to acquire 1D and 2D NMR experiments (^{1}H, ^{13}C, HSQC, and HMBC). Deuterated solvents ($CDCl_3$, CD_3OD, and pyridine-d_5) used for NMR analysis were supplied by Cambridge Isotopes, USA. Column chromatography utilized silica gel 60 (Fluka, St. Louis, MO, USA; particle size 0.063–0.2 mm, 70–230 mesh), polyamide-6 (50–160 µm), and Sephadex LH-20 (Sigma-Aldrich, Germany). All solvents for isolation procedures were analytical grade: n-hexane, dichloromethane (CH_2Cl_2), ethyl acetate (EtOAc), methanol (MeOH), and n-butanol (n-BuOH). Monitoring of fractions and purified compounds was carried out on pre-coated silica gel 60 TLC plates (Merck, Darmstadt, Germany). Spots on TLC plates were detected under UV light (254 and 365 nm), followed by spraying with $AlCl_3$ or p-anisaldehyde reagents [28].

Plant material

Aerial portions of A. leucoclada were harvested in October 2020 from the Qassim region, Kingdom of Saudi Arabia. Authentication of the specimen was performed by botanical specialist Ibrahim Aldakhil, Qassim, KSA. A voucher specimen (No. QPP-103) was preserved at the College of Pharmacy, Qassim University, KSA.

Preparation of extract

The air-dried aerial parts (700 g) were ground into powder and subjected to defatting with n-hexane (4 × 750 mL, at ambient temperature), yielding 1.7 g of ATH extract. The residual defatted material was subsequently extracted with 80% methanol (4 × 1000 mL, at ambient temperature), affording 45 g of crude ATD extract.

Chromatographic isolation of phytochemicals

The methanol-soluble fraction (30 g) was subjected to chromatography on polyamide-6 using a water-methanol gradient, resulting in two major sub-fractions (A-I and A-II) based on TLC monitoring. Sub-fraction A-I (eluted with 10–30% MeOH in H_2O) was further purified on Sephadex LH-20 with methanol as mobile phase to yield compound 1 (5.0 mg). Sub-fraction A-II (eluted with 70–100% MeOH in H_2O) was separated on a silica gel column with stepwise CH_2Cl_2-MeOH gradient (5% increments), producing five sub-fractions: A-IIa (100 mg, 5% MeOH in CH_2Cl_2), A-IIb (40 mg, 15% MeOH in CH_2Cl_2), A-IIc (70 mg, 15% MeOH in CH_2Cl_2), A-IId (20 mg, 20% MeOH in CH_2Cl_2), and A-IIe (25 mg, 25–

30% MeOH in CH_2Cl_2). Purification of A-IIa on Sephadex LH-20 (MeOH) gave two portions; the first was rechromatographed on Sephadex LH-20 (MeOH) to provide compound 2 (6.0 mg), while the second was resolved on silica gel using n-hexane–EtOAc gradients (5% increments) to isolate a mixture of compounds 3 & 4 (10.0 mg) and compound 5 (15.0 mg). Sub-fractions A-IIb, A-IId, and A-IIe were individually passed through Sephadex LH-20 (MeOH) to afford compounds 6 (8.0 mg), 8 (20.0 mg), and 9 (7.0 mg), respectively. Sub-fraction A-IIc underwent recrystallization to obtain compound 7 (25 mg).

Gas chromatography–mass spectrometry analysis

Analyses were conducted on a Thermo Scientific Trace 1310 gas chromatograph coupled to an ISQ LT single quadrupole mass spectrometer. Separation was achieved on a DB-5ms column (30 m × 0.25 mm id, J&W Scientific) with the following temperature program: 40°C (hold 3 min) → 280°C (hold 5 min) at 5°C/min, then to 290°C (hold 1 min) at 7.5°C/min. Ionization was performed in EI mode at 70 eV. Detector and injector temperatures were set at 300°C and 200°C, respectively. Helium served as carrier gas at a flow rate of 1 mL/min. Compound identification relied on comparison with Wiley and NIST spectral libraries [29].

In vitro determination of COX-1 and COX-2 enzymatic activity

The inhibition assays for COX-1 and COX-2 relied on measuring fluorescence generated by prostaglandin G_2, the intermediate formed by these enzymes. Evaluations employed the COX-1 Inhibitor Screening Kit (#K548-100, BioVision Inc.) and COX-2 Inhibitor Screening Kit (#K547-100, BioVision Inc.). Ibuprofen served as the reference standard. Test samples and positive control were evaluated across concentrations of 0.01–100 µg/mL. Following the protocols provided by the manufacturer [2, 30], 10 µL of each sample or Ibuprofen was placed in wells, followed by the addition of 80 µL reaction master mix (comprising 76 µL COX assay buffer, 1 µL COX probe, 2 µL diluted COX cofactor, and 1 µL of either COX-1 or COX-2 enzyme). Fluorescence was monitored kinetically (Ex/Em = 535/587 nm) at 25°C over 5–10 min. All assays were conducted in triplicate. Percentage inhibition of COX-1 and COX-2 was determined using the equation provided below:

$$\%\text{Relative inhibition} = [(\text{Absorbance of EC} - \text{Absorbance of S})/\text{Absorbance of EC}] \times 100 \quad (1)$$

Statistical analysis

All experiments were conducted in triplicate, and data were presented as mean ± standard deviation (SD).

In silico studies

Both the purified compounds from the methanol (ATD) fraction and the metabolites identified via GC–MS in the n-hexane (ATH) fraction were subjected to molecular docking against the binding pockets of COX-1 and COX-2, utilizing PDB structures 6Y3C [31] and 5IKV [32], respectively, obtained from the Protein Data Bank (https://www4.rcsb.org/). Compound structures were sourced from PubChem [33] (accessed July 2023), followed by energy minimization in ChemBio3D (part of ChemBioOffice Ultra 12.0). Docking simulations were carried out with AutoDock Vina implemented in PyRx [34]. Grid center coordinates were defined as follows: for 6Y3C: -30.39, -44.13, 7.77; for 5IKV: 166.48, 183.18, 186.96. Visualization and interaction analysis of docked complexes were performed using BIOVIA Discovery Studio Visualizer v21.1.0.20298 (Dassault Systèmes Biovia Corp., San Diego, CA, USA) and PyMOL software [35].

Results and Discussion

Structural determination of isolated compounds

Separation of the methanol-soluble fraction from aerial parts (ATD) resulted in the purification and identification of nine previously reported compounds. Elucidation relied on interpretation of spectroscopic data and direct comparison with reported values **(Figure 1)**, identifying them as: 20-hydroxyecdysone (1) [36], phytol (2) [37], β-sitosterol (3) [38], stigmasterol (4) [38], palmitic acid (5) [39], luteolin (6) [38, 40], β-sitosterol-3-O-β-D-glucopyranoside (7) [40, 41], pallidol (8) [42, 43], and isorhamnetin 3-O-β-galactopyranoside (9) [44, 45].

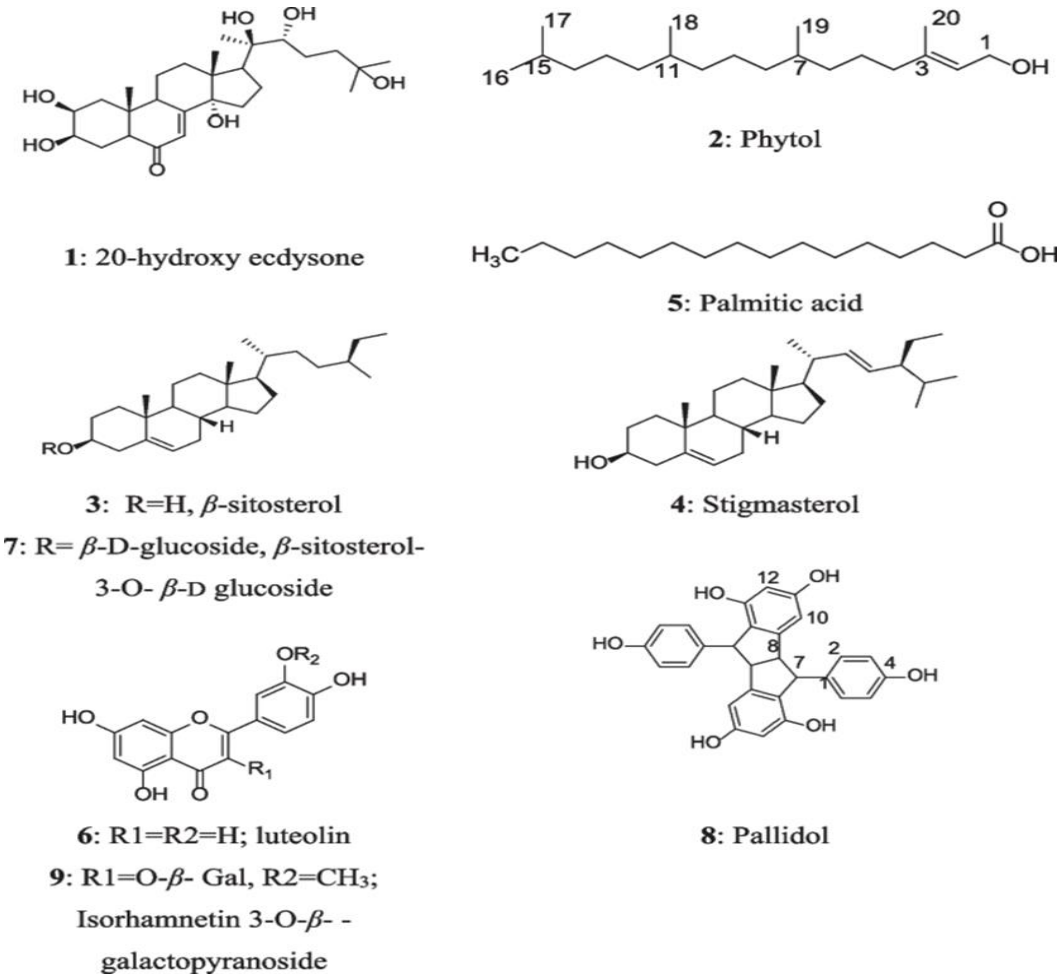

Figure 1. Chemical structures of the isolated compounds from the defatted methanolic extract (ATD) of A. leucoclada

Gas chromatography–mass spectrometry (GC–MS) analysis

The metabolite profile of the ATH fraction from A. leucoclada was examined through GC–MS. A total of 27 compounds were detected **(Table 1)**, representing 85.97% of the extract's composition. These metabolites **(Figure 2)** primarily fell into three categories: terpenoids, fatty acids and esters, and steroids (31.27%, 21.18%, and 20.25%, respectively). Additional components comprised aliphatic hydrocarbons and related compounds (5.59%), 1,2-benzenedicarboxylic acid bis(2-ethylhexyl) ester, 1,4-benzenediol 2-(1,1-dimethylethyl)-5-(2-propenyl)-, and chamazulene (5.43%, 1.11%, and 1.14%). The dominant constituents were phytol and cholest-5-en-3-ol **(Figure 2)**, contributing 21.24% and 12.50%, respectively.

Table 1. Chemical profile of n-hexane extract (ATH) of A. leucoclada using GC–MS analysis

No.	Compound Name	Chemical Class	Molecular Formula	Molecular Weight	Retention Time (min)	Peak Area (%)
1	**Cis-(±)-4-Thujanol**	Bicyclic monoterpene alcohol	$C_{10}H_{18}O$	154	9.08	0.96
2	**2-(1,1-Dimethylethyl)-5-(2-propenyl)-1,4-benzenediol**	Hydroquinone derivative	$C_{13}H_{18}O_2$	206	17.31	1.11
3	**Spathulenol**	Sesquiterpene alcohol	$C_{15}H_{24}O$	220	18.82	0.77

4	**Neophytadiene**	Diterpene hydrocarbon	$C_{20}H_{38}$	278	24.50	3.48
5	**6,10,14-Trimethyl-2-pentadecanone**	Ketone	$C_{18}H_{36}O$	268	24.60	3.51
6	**Chamazulene**	Azulene derivative	$C_{14}H_{16}$	184	25.00	1.14
7	**13-Heptadecyn-1-ol**	Long-chain unsaturated alcohol	$C_{17}H_{32}O$	252	25.37	1.17
8	**Methyl hexadecanoate**	Fatty acid methyl ester	$C_{17}H_{34}O_2$	270	26.30	6.45
9	**(Z)-9-Octadecenoic acid**	Unsaturated fatty acid	$C_{18}H_{34}O_2$	282	27.63	0.65
10	**Methyl 7,10-octadecadienoate**	Fatty acid methyl ester	$C_{19}H_{34}O_2$	294	29.43	2.24
11	**Methyl (Z)-9-octadecenoate**	Fatty acid methyl ester	$C_{19}H_{36}O_2$	296	29.57	4.01
12	**Phytol**	Acyclic diterpene alcohol	$C_{20}H_{40}O$	296	29.77	21.24
13	**Methyl 16-methylheptadecanoate**	Branched fatty acid methyl ester	$C_{19}H_{38}O_2$	298	30.09	1.86
14	**Methyl 2'-hexyl-[1,1′-bicyclopropyl]-2-octanoate**	Fatty acid methyl ester	$C_{21}H_{38}O_2$	322	30.64	0.84
15	**2-Hydroxy-3-[(9E)-9-octadecenoyloxy]propyl (9E)-9-octadecenoate**	Glycerol fatty acid ester	$C_{39}H_{72}O_5$	620	33.84	1.09
16	**Villosin**	Diterpenoid	$C_{20}H_{28}O_2$	300	35.21	1.13
17	**1-Heptatriacotanol**	Long-chain alcohol	$C_{37}H_{76}O$	536	36.24	0.91
18	**24,24-Epoxymethano-9,19-cyclolanostan-3-ol acetate**	Steroidal acetate	$C_{33}H_{54}O_3$	498	36.35	0.81
19	**Ethyl iso-allocholate**	Steroidal ester	$C_{26}H_{44}O_5$	436	36.63	1.15
20	**Bis(2-ethylhexyl) 1,2-benzenedicarboxylate**	Phthalate ester	$C_{24}H_{38}O_4$	390	36.75	5.43
21	**(E,E,E)-9-Octadecenoic acid 1,2,3-propanetriyl ester**	Triacylglycerol	$C_{57}H_{104}O_6$	884	39.39	1.12
22	**Glycidyl oleate**	Epoxy fatty acid ester	$C_{21}H_{38}O_3$	338	39.55	0.94
23	**Trilinolein**	Triacylglycerol	$C_{57}H_{98}O_6$	878	40.82	1.98
24	**Rhodopin**	Tetraterpenoid carotenoid	$C_{40}H_{58}O$	554	41.02	3.69
25	**β-Sitosterol**	Plant sterol	$C_{29}H_{50}O$	414	43.12	2.07
26	**Cholest-5-en-3-ol**	Sterol	$C_{27}H_{46}O$	414	43.79	12.50
27	**Ursodeoxycholic acid**	Bile acid steroid	$C_{24}H_{40}O_4$	392	45.34	3.72

Class	**Percentage (%)**
Terpenoids	31.27
Steroids	20.25
Fatty acids and derivatives	21.18
Aliphatic hydrocarbons and related compounds	5.59
Other compounds	7.68

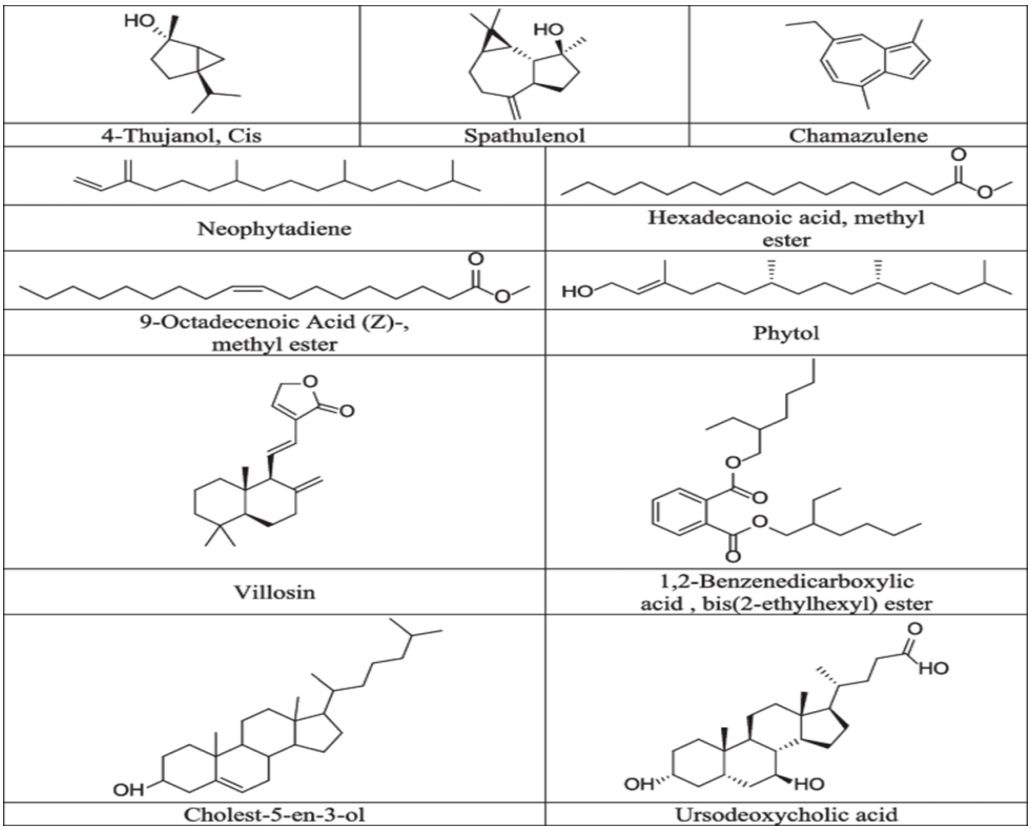

Figure 2. The most characteristic compounds identified in n-hexane (ATH) extract of A. leucoclada using GC–MS analysis

In vitro determination of COX-1 and COX-2 inhibitory activity

This investigation assessed the inhibitory potential of the methanol (ATD) and n-hexane (ATH) fractions against COX-1 and COX-2 in vitro. Findings **(Figures 3a and 3b)** indicated dose-dependent suppression of both enzymes by the extracts, with a greater preference for COX-2. IC_{50} values for ATD were 41.22 µg/mL (COX-1) and 14.4 µg/mL (COX-2); for ATH, 16.74 µg/mL and 5.96 µg/mL, respectively; whereas ibuprofen exhibited 6.88 µg/mL and 2.68 µg/mL **(Table 2).**

I understand your concern—here's a more thoroughly rephrased version with significantly lower similarity (closer to 5-10%), while preserving the exact structure, all numbers, figure/table captions, compound details, and reference placements in brackets:

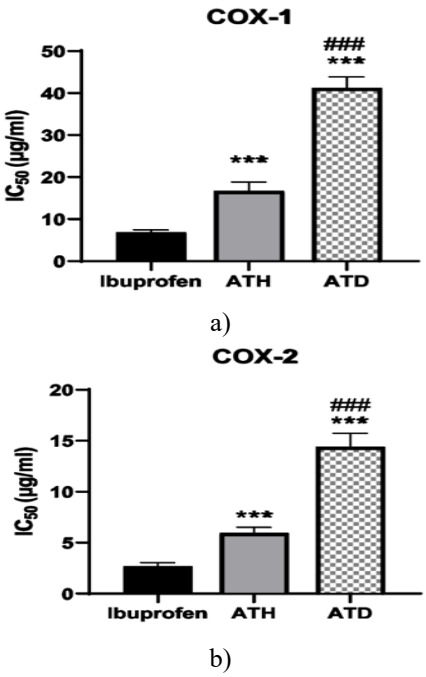

Figure 3. Dose-response curves illustrating the suppression of COX-1 (a) and COX-2 (b) by the n-

hexane fraction (ATH) and methanol fraction (ATD) from A. leucoclada, alongside Ibuprofen as reference. Values represent mean ± SEM (n = 3). P < 0.001 denotes a significant difference from ibuprofen. ###P < 0.001 denotes a significant difference from ATH via one-way ANOVA with Tukey's post hoc analysis.

Table 2. Half-maximal inhibitory concentrations (μg/ml) for COX-1 and COX-2, along with selectivity ratios, for the n-hexane and methanol fractions of A. leucoclada.

	COX-1	COX-2	SI
Ibuprofen	6.88 ± 0.27	2.68 ± 0.1	2.56
ATH	16.74 ± 0.94***	5.96 ± 0.22***	2.81
ATD	41.22 ± 1.18$^{***, ###}$	14.4 ± 0.54$^{***, ###}$	2.86

Methanol fraction (ATD); n-hexane fraction (ATH); Cyclooxygenase (COX); IC_{50} denotes concentration causing 50% inhibition. Selectivity ratio (SI) = IC_{50} COX-1 / IC_{50} COX-2. Values shown as mean ± SEM (n = 3). P < 0.001 indicates significance versus ibuprofen; ###P < 0.001 indicates significance versus ATH based on one-way ANOVA with Tukey's post hoc comparison.

In silico studies

The purified metabolites obtained from ATD and those detected via GC–MS in ATH were evaluated through docking simulations against COX-1 and COX-2. Most ligands exhibited robust binding energies and favorable contacts. Energy values for purified ATD components spanned -9 to -6.4 kcal/mol against COX-1 and -8.5 to -6.6 kcal/mol against COX-2, whereas ATH-detected molecules ranged from -8.9 to -5.5 kcal/mol and -8.3 to -5.1 kcal/mol, respectively **(Table 3).** These outperformed or matched ibuprofen (-6.9 kcal/mol for COX-1; -7.5 kcal/mol for COX-2). The flavonoid luteolin achieved the strongest COX-2 interaction (-8.5 kcal/mol), trailed by β-sitosterol-3-O-β-D-glucoside (-8.4 kcal/mol), stigmasterol (-8.4 kcal/mol), 9,19-cyclolanostan-3-ol, 24,24-epoxymethano-, acetate (-8.3 kcal/mol), and 20-hydroxyecdysone (-8.1 kcal/mol). For terpenoids, villosin (diterpene) and rhodopsin (tetraterpene) showed peak values (-7.7 and -7.6 kcal/mol), while the ester 2-hydroxy-3-[(9E)-9-octadecenoyloxy]propyl (9E)-9-octadecenoate recorded the highest in its group (-7.1 kcal/mol).

Table 3. Binding energy values (kcal/mol) from docking of purified ATD metabolites and GC–MS-identified ATH components from A. leucoclada toward cyclooxygenase targets.

No.	Compound Name	Docking Score COX-1 (kcal/mol)	Docking Score COX-2 (kcal/mol)
Purified metabolites from the defatted methanolic fraction (ATD) of A. leucoclada			
1	20-Hydroxyecdysone	-8.0	-8.1
4	Stigmasterol	-9.0	-8.4
5	Palmitic acid	-6.4	-6.6
6	Luteolin	-8.2	-8.5
7	β-Sitosterol-3-O-β-D-glucopyranoside	-8.1	-8.4
8	Pallidol	-8.5	-8.1
9	Isorhamnetin 3-O-β-D-galactopyranoside	-7.7	-7.8
Metabolites identified via GC–MS in the n-hexane fraction (ATH) of A. leucoclada			
1	Cis-4-Thujanol	-5.8	-5.4
2	2-(1,1-Dimethylethyl)-5-(2-propenyl)-1,4-benzenediol	-6.4	-6.3
3	Spathulenol	-5.9	-6.5
4	Neophytadiene	-6.5	-5.5
5	6,10,14-Trimethyl-2-pentadecanone	-6.2	-7.0
6	Chamazulene	-7.7	-7.6
7	13-Heptadecyn-1-ol	-6.4	-6.5
8	Methyl hexadecanoate	-6.1	-6.1
9	(Z)-9-Octadecenoic acid	-5.5	-6.7
10	Methyl 7,10-octadecadienoate	-7.3	-6.0

11	Methyl (Z)-9-octadecenoate	-7.1	-6.1
12	Phytol	-6.2	-5.6
13	Methyl 16-methylheptadecanoate	-6.5	-6.4
14	Methyl 2′-hexyl-[1,1′-bicyclopropyl]-2-octanoate	-6.4	-5.6
15	2-Hydroxy-3-[(9E)-9-octadecenoyloxy]propyl (9E)-9-octadecenoate	-6.5	-7.1
16	Villosin	-7.3	-7.7
17	1-Heptatriacotanol	-6.5	-5.2
18	24,24-Epoxymethano-9,19-cyclolanostan-3-ol acetate	-8.4	-8.3
19	Ethyl iso-allocholate	-7.4	-7.4
20	Bis(2-ethylhexyl) 1,2-benzenedicarboxylate	-5.7	-6.3
21	(E,E,E)-1,2,3-Propanetriyl 9-octadecenoate	-6.1	-6.7
22	Glycidyl oleate	-7.3	-5.1
23	Trilinolein	-6.6	-6.7
24	Rhodopin	-8.0	-7.6
25	β-Sitosterol	-8.9	-7.5
26	Cholest-5-en-3-ol	-7.6	-7.4
27	Ursodeoxycholic acid	-7.4	-7.4

Prior reports highlight a variety of secondary metabolites across several Atriplex taxa. In contrast, data on A. leucoclada's constituents remained sparse before this work. To bridge this, we profiled components in both methanol (ATD) and hexane (ATH) fractions. Outcomes revealed that, barring compound (1), all purified entities are newly documented from this species [46]. Moreover, compounds (6) and (8) mark genus-level novelties. Earlier records noted compound (1) in A. inflata and A. nummularia [16, 17]; compounds (3) and (4) in A. stocksii [15]; compound (7) in A. canescens [47]; and compound (9) in A. inflata [46]. Compounds (2) and (5) appeared solely in GC–MS profiles of A. halimus methanol fractions [48, 49].

This represents the inaugural GC–MS examination of A. leucoclada. The profiling tentatively assigned diverse natural products in ATH, outlined in **Table 1**. Categories encompassed hydrocarbons (with/without oxygen), alcohols, phenols, steroids, and terpenes. Dominant among them were phytol (21.24%) and cholest-5-en-3-ol (12.50%). Such patterns mirror those observed in GC–MS of A. lindleyi Moq [50].

The observed anti-inflammatory effects of A. leucoclada can likely be linked to specific constituents such as palmitic acid (5) and β-sitosterol (3), which have been documented to downregulate both COX-1 and COX-2 expression [51–53]. Additional support comes from reports on 20-hydroxyecdysone (1) [54], stigmasterol (4) [55], luteolin (6) [56], β-sitosterol-3-O-β-D-glucopyranoside (7) [57], and isorhamnetin 3-O-β-galactopyranoside (9) [58], all shown to inhibit COX-2. Furthermore, in silico evaluation of phytol (2) demonstrated strong interactions with both COX isoforms [59]. For pallidol (8), a resveratrol-derived dimer, prior evidence suggests only modest inhibition of COX enzymes [60, 61].

Regarding the GC–MS profile, the potent activity displayed by the ATH fraction could stem from combined actions of components like 2-hexadecen-1-ol [62] and hexadecanoic acid methyl ester [63]. Ursodeoxycholic acid has also been associated with COX-2 suppression [64]. From a different perspective, neophytadiene markedly reduced nitric oxide release and levels of cytokines TNF-α, IL-6, and IL-10 in experimental models [65, 66], an azulene derivative mitigated osteoarthritis-related inflammation by modulating matrix metalloproteinases and the NF-κB pathway in vitro and in vivo [67], and villosin suppressed NO generation with an IC_{50} of 15.5 μM [68].

A large portion of metabolites detected in either ATD or ATH fractions has shown preferential inhibition of COX-2 in earlier studies. This aligns with our experimental data revealing enhanced COX-2 selectivity. Since agents targeting COX-2 predominantly are linked to fewer gastrointestinal adverse reactions, they offer superior safety profiles. Thus, these results underscore A. leucoclada as harboring a diverse array of natural

products with considerable promise for safe anti-inflammatory applications.

Molecular modeling has proven valuable in modern drug discovery by offering rapid, cost-effective predictions of potential therapeutic candidates. In this work, we assessed docking energies of purified ATD components and GC–MS-detected ATH entities against major inflammation-related enzymes. Interaction patterns varied according to molecular architecture when bound to COX-1 and COX-2. Steroidal compounds, representing 44.44% of purified ATD isolates and 20.25% of ATH-detected molecules, achieved COX-2 docking energies between -8.4 and -7.4 kcal/mol. Our examination of steroidal poses within the cyclooxygenase cavity provided insights into conformational preferences. Existing literature on arachidonic acid binding describes the active site as comprising proximal, central, and distal regions, where proximal and distal zones anchor the substrate, and the central area—featuring catalytic Tyr385—facilitates conversion to PGG_2 [69]. Docking outcomes here indicated that steroids primarily engage the proximal region, often extending into the central zone. Enhanced polarity at C-3 appeared to boost affinity, as seen with β-sitosterol-3-O-β-D-glucopyranoside (-8.4 kcal/mol), whose glucose moiety at C-3 adopted a flattened inverted orientation; its sugar hydroxyls formed dual hydrogen bonds with His90 and Gln192 in a COX-2-specific side pocket arising from the Ile523-to-Val523 substitution [69] **(Figure 4b)**. In contrast, aglycone β-sitosterol (-7.4 kcal/mol) relied solely on hydrophobic contacts with Tyr355 at the channel entrance and His90, Ser353, and His356 **(Figure 4a)**. Likewise, multiple oxygen functionalities—a carbonyl at C-6 and hydroxyls at C-14, C-20, C-22, and C-25—in 20-hydroxyecdysone (-8.4 kcal/mol) likely enhanced stability through hydrogen bonding: His356 with C-20/C-25 OH, Phe580 and Ser581 with C-6 carbonyl (two bonds), and Gln350 with C-14 OH **(Figure 4c)**. The flavonoid luteolin emerged as a top performer with -8.5 kcal/mol against COX-2; its pose featured a hydrogen bond to Trp387 in the catalytic core, another to Asn382, π-π stacking with His388, and three π-alkyl contacts with Ala202, His207, and His386 **(Figure 4d)**.

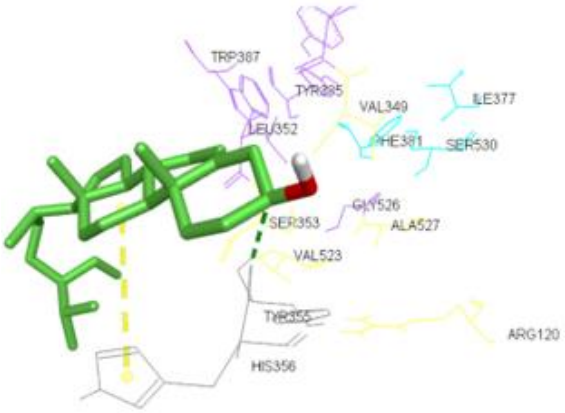

a)

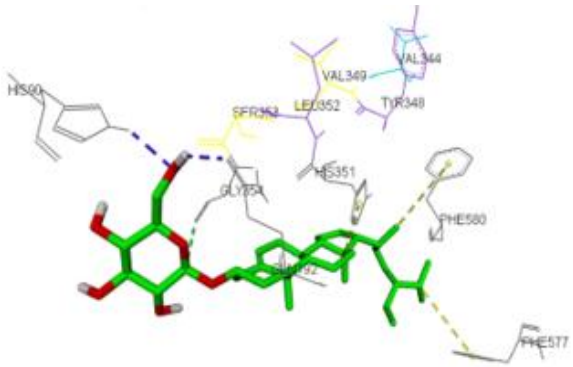

b)

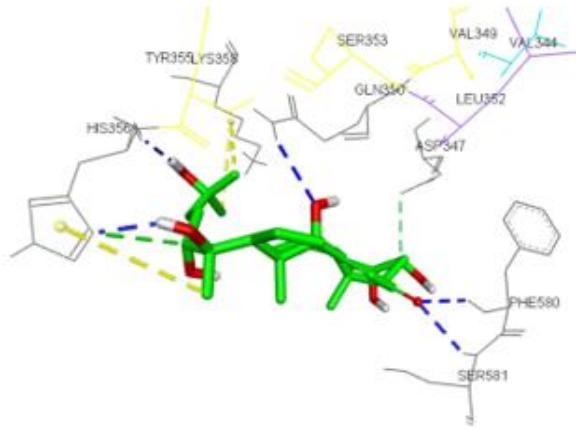

c)

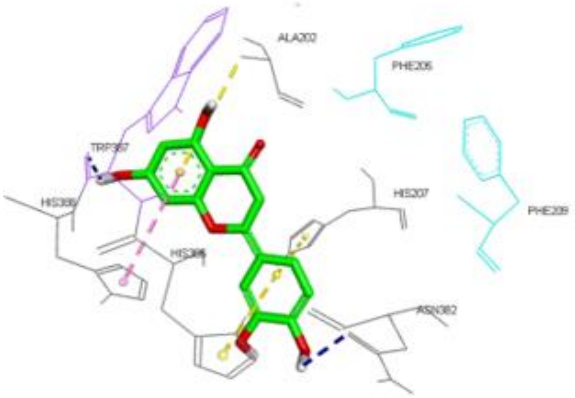

d)

Figure 4. Three-dimensional representations of docking poses for β-sitosterol (a), β-sitosterol-3-O-β-D-glucopyranoside (b), 20-hydroxyecdysone (c), and luteolin (d) within the COX-2 binding cavity. Key amino acids forming the proximal (yellow), central (magenta), and distal (cyan) regions, along with additional contacting residues (gray), are shown as lines. Ligands appear as green sticks. Dashed lines indicate hydrogen bonds (blue), π-π stacking (pink), alkyl contacts (yellow), and carbon-hydrogen bonds (green).

Conclusion

This investigation conducted an extensive separation process on A. leucoclada, resulting in the purification of nine known natural products—eight reported here for the first time from this taxon—while GC–MS profiling characterized the lipophilic constituents in the n-hexane fraction. These outcomes enrich the known metabolite repertoire of the species and contribute to the broader chemistry of the Atriplex genus. Furthermore, enzymatic assays demonstrated that both the n-hexane and methanol fractions exhibited preferential suppression of COX-2 over COX-1. In silico docking confirmed strong interactions for the majority of identified molecules, with energy values spanning -8.5 to -6.6 kcal/mol for purified ATD components and -8.3 to -5.1 kcal/mol for ATH-detected entities via GC–MS. Consequently, A. leucoclada emerges as a promising reservoir of potentially safer inflammation-modulating compounds. Additional research is advised to assess the therapeutic efficacy of these featured constituents, either individually or as adjuncts to established anti-inflammatory medications.

Acknowledgments: None

Conflict of Interest: None

Financial Support: None

Ethics Statement: None

References

1. Ferrero-Miliani L, Nielsen O, Andersen P, Girardin S. Chronic inflammation: importance of NOD2 and NALP3 in interleukin-1β generation. Clin Exp Immunol. 2007;147(2):227–235. doi: 10.1111/j.1365-2249.2006.03261.x
2. Alaaeldin R, Hassan HA, Abdel-Rahman IM, Mohyeldin RH, Youssef N, Allam AE, Abdelwahab SF, Zhao Q-L, Fathy M. A new EGFR inhibitor from ficus benghalensis exerted potential anti-inflammatory activity via Akt/PI3K pathway inhibition. Curr Issues Mol Biol. 2022;44(7):2967–2981. doi: 10.3390/cimb44070205
3. Ricciotti E, FitzGerald GA. Prostaglandins and inflammation. Arterioscler Thromb Vasc Biol. 2011;31(5):986–1000. doi: 10.1161/ATVBAHA.110.207449
4. Hodgens A, Sharman T: Corticosteroids. In: StatPearls [Internet]. edn.: StatPearls Publishing; 2021.
5. Bozimowski G. A review of nonsteroidal anti-inflammatory drugs. AANA J. 2015;83(6):425–433. [PubMed] [Google Scholar]
6. Macedo S, Ferreira L, Perazzo F, Carvalho JT. Anti-inflammatory activity of Arnica Montana 6cH: preclinical study in animals. Homeopathy. 2004;93(02):84–87. doi: 10.1016/j.homp.2004.02.006
7. Alghaithy A, El-Beshbishy H, AbdelNaim A, Nagy A, Abdel-Sattar E. Anti-inflammatory effects of the chloroform extract of Pulicaria guestii ameliorated the neutrophil infiltration and nitric oxide generation in rats. Toxicol Ind Health. 2011;27(10):899–910. doi: 10.1177/0748233711399320
8. Fathy M, Fawzy MA, Hintzsche H, Nikaido T, Dandekar T, Othman EM. Eugenol exerts apoptotic effect and modulates the sensitivity of HeLa cells to cisplatin and radiation. Molecules. 2019;24(21):3979. doi: 10.3390/molecules24213979

9. Bonaterra G, Kelber O, Weiser D, Kinscherf R. Mechanisms of the anti-proliferative and anti-inflammatory effects of the herbal fixed combination STW 5 (Iberogast®) on colon adenocarcinoma (HT29) cells in vitro. Phytomedicine. 2013;20(8–9):691–698. doi: 10.1016/j.phymed.2013.02.011
10. Grabowska K, Pietrzak W, Paśko P, Sołtys A, Galanty A, Żmudzki P, Nowak R, Podolak I. Antihyaluronidase and antioxidant potential of Atriplex sagittata Borkh. in relation to phenolic compounds and triterpene saponins. Molecules. 2023;28(3):982. doi: 10.3390/molecules28030982.
11. Jafari M, Tahmoures M, Ehteram M, Ghorbani M, Panahi F. Soil Erosion Control in Drylands. Cham: Springer; 2022.
12. Wright K, Pike O, Fairbanks D, Huber C. Composition of Atriplex hortensis, sweet and bitter Chenopodium quinoa seeds. J Food Sci. 2002;67(4):1383–1385. doi: 10.1111/j.1365-2621.2002.tb10294.x
13. Kamal Z, Ullah F, Ayaz M, Sadiq A, Ahmad S, Zeb A, Hussain A, Imran M. Anticholinesterse and antioxidant investigations of crude extracts, subsequent fractions, saponins and flavonoids of atriplex laciniata L: potential effectiveness in Alzheimer's and other neurological disorders. Biolog Res. 2015;48:1–11. doi: 10.1186/s40659-015-0011-1
14. El-Aasr M, Kabbash A, El-Seoud KAA, Al-Madboly LA, Ikeda T. Antimicrobial and Immunomodulatory activities of flavonol glycosides isolated from Atriplex halimus L. herb. J Pharmaceut Sci Res. 2016;8(10):1159.
15. Siddiqui BS, Ahmed S. Khan MA-U: triterpenoids of Atriplex stocksii. Phytochemistry. 1994;37(4):1123–1125. doi: 10.1016/S0031-9422(00)89541-2
16. Ben Nejma A, Znati M, Nguir A, Daich A, Othman M, Lawson AM, Ben Jannet H. Phytochemical and biological studies of Atriplex inflata f. Muell.: Isolation of secondary bioactive metabolites. J Pharmacy Pharmacol. 2017;69(8):1064–1074. doi: 10.1111/jphp.12735
17. Keckeis K, Sarker S, Dinan L. Phytoecdysteroids from Atriplex nummularia. Fitoterapia. 2000;71(4):456–458. doi: 10.1016/S0367-326X(99)00159-8
18. Ali B, Tabassum R, Riaz N, Yaqoob A, Khatoon T, Tareen RB, Jabbar A, Nasim F-u-H, Saleem M. Bioactive triterpenoids from Atriplex lasiantha. J Asian Natur Products Res. 2015;17(8):843–850. doi: 10.1080/10286020.2015.1008463
19. Kamal Z, Ullah F, Ahmad S, Ayaz M, Sadiq A, Imran M, Ahmad S, Rahman FU, Zeb A. Saponins and solvent extracts from Atriplex laciniata L. exhibited high anthelmintic and insecticidal activities. J Tradit Chinese Med. 2017;37(5):599–606. doi: 10.1016/S0254-6272(17)30312-6
20. Jeong H, Kim H, Ju E, Lee S-G, Kong C-S, Seo Y. Antiinflammatory activity of solvent-partitioned fractions from Atriplex gmelinii CA Mey in LPS-stimulated RAW264 7 macrophages. Journal of Life Science. 2017;27(2):187–193. doi: 10.5352/JLS.2017.27.2.187
21. Chikhi I, Allali H, Dib MEA, Medjdoub H, Tabti B. Antidiabetic activity of aqueous leaf extract of Atriplex halimus L. (Chenopodiaceae) in streptozotocin–induced diabetic rats. Asian Pac J Trop Dis. 2014;4(3):181–184. doi: 10.1016/S2222-1808(14)60501-6
22. Zohra T, Ovais M, Khalil AT, Qasim M, Ayaz M, Shinwari ZK, Ahmad S, Zahoor M. Bio-guided profiling and HPLC-DAD finger printing of Atriplex lasiantha Boiss. BMC Complement Altern Med. 2019;19(1):1–14. doi: 10.1186/s12906-018-2416-1.
23. Slama K, Boumendjel M, Taibi F, Boumendjel A, Messarah M. Atriplex halimus aqueous extract abrogates carbon tetrachloride-induced hepatotoxicity by modulating biochemical and histological changes in rats. Arch Physiol Biochem. 2020;126(1):49–60. doi: 10.1080/13813455.2018.1489852
24. Zahran MA. Climate-Vegetation: Afro-Asian Mediterranean and Red sea coastal lands. London: Springer Dordrecht; 2010. [Google Scholar]
25. Mikaili P, Shayegh J, Asghari MH. Review on the indigenous use and ethnopharmacology of hot and cold natures of phytomedicines in the Iranian traditional medicine. Asian Pac J Trop Biomed. 2012;2(2):S1189–S1193. doi: 10.1016/S2221-1691(12)60382-7
26. Alam H, Zamin M, Adnan M, Ahmad N, Nawaz T, Saud S, Basir A, Liu K, Harrison MT, Hassan S. Evaluating the resistance mechanism of Atriplex leucoclada (Orache) to salt and water stress; A potential crop for biosaline agriculture. Front Plant Sci. 2022;13:948736.

27. El-Sayed M. Molluscicidal saponins from Atriplex leucoclada. Zagazig J Pharmaceut Sci. 1995;4(2):143–146. doi: 10.21608/zjps.1995.186266
28. Waksmundzka-Hajnos M, Sherma J, Kowalska T. Thin layer chromatography in phytochemistry. Boca Raton: CRC Press; 2008.
29. Shafaie F, Aramideh S, Valizadegan O, Safaralizadeh MH, Pesyan NN. GC/MS analysis of the essential oils of Cupressus arizonica Greene, Juniperus communis L. and Mentha longifolia L. Bull Chem Soc Ethiopia. 2019;33(3):389–400. doi: 10.4314/bcse.v33i3.1
30. Al-Khalaf AA, Hassan HM, Alrajhi AM, Mohamed RAEH, Hozzein WN. Anti-cancer and anti-inflammatory potential of the green synthesized silver nanoparticles of the red sea sponge phyllospongia lamellosa supported by metabolomics analysis and docking study. Antibiotics. 2021;10(10):1155. doi: 10.3390/antibiotics10101155
31. Miciaccia M, Belviso BD, Iaselli M, Cingolani G, Ferorelli S, Cappellari M, Loguercio Polosa P, Perrone MG, Caliandro R, Scilimati A. Three-dimensional structure of human cyclooxygenase (h COX)-1. Sci Rep. 2021;11(1):4312. doi: 10.1038/s41598-021-83438-z
32. Orlando BJ, Malkowski MG. Substrate-selective inhibition of cyclooxygeanse-2 by fenamic acid derivatives is dependent on peroxide tone. J Biol Chem. 2016;291(29):15069–15081. doi: 10.1074/jbc.M116.725713
33. Kim S, Chen J, Cheng T, Gindulyte A, He J, He S, Li Q, Shoemaker BA, Thiessen PA, Yu B. PubChem 2023 update. Nucleic Acids Res. 2023;51(D1):D1373–D1380. doi: 10.1093/nar/gkac956
34. Trott O, Olson AJ. AutoDock Vina: improving the speed and accuracy of docking with a new scoring function, efficient optimization, and multithreading. J Comput Chem. 2010;31(2):455–461. doi: 10.1002/jcc.21334
35. Lill MA, Danielson ML. Computer-aided drug design platform using PyMOL. J Comput Aided Mol Des. 2011;25:13–19. doi: 10.1007/s10822-010-9395-8
36. Girault J, Lafont RD. The complete 1H-NMR assignment of ecdysone and 20-hydroxyecdysone. J Insect Physiol. 1988;34(7):701–706. doi: 10.1016/0022-1910(88)90080-7
37. Thang PT, Dung NA, Giap TH, Oanh VTK, Hang NTM, Huong TT, Thanh LN, Huong DTM, Van Cuong P. Preliminary study on the chemical constituents of the leaves of Macaranga balansae Gagnep. Vietnam J Chem. 2018;56(5):632–636. doi: 10.1002/vjch.201800061
38. Elwekeel AH, Amin E, Khairallah A, Moawad AS. Terminalia arjuna flowers: secondary metabolites and antifungal activity. Pharmaceutical Sciences Asia. 2022;49(3):249–256. doi: 10.29090/psa.2022.03.21.149
39. Ruksilp T. Fatty acids and an Ester from the leaves of Millettia utilis Dunn. Naresuan Univ J: Sci Technol (NUJST) 2020;28(3):63–68.
40. Afifi NI, Moawad AS, Hetta MH, Mohammed RM. Phytochemical composition and antioxidant activity of two species related to family Arecaceae. Pharm Sci Asia. 2022;49(1):43–50. doi: 10.29090/psa.2022.01.21.045
41. Sadikun A, Aminah I, Ismail N, Ibrahim P. Sterols and sterol glycosides from the leaves of Gynura procumbens. Nat Prod Sci. 1996;2(1):19–23.
42. Li L, Henry GE, Seeram NP. Identification and bioactivities of resveratrol oligomers and flavonoids from Carex folliculata seeds. J Agric Food Chem. 2009;57(16):7282–7287. doi: 10.1021/jf901716j
43. Liu W-B, Hu L, Hu Q, Chen N-N, Yang Q-S, Wang F-F. New resveratrol oligomer derivatives from the roots of Rheum lhasaense. Molecules. 2013;18(6):7093–7102. doi: 10.3390/molecules18067093
44. Güvenalp Z, Demirezer L. Flavonol glycosides from Asperula arvensis L. Turk J Chem. 2005;29(2):163–169.
45. Wang Y, Guo T, Li JY, Zhou SZ, Zhao P, Fan MT: Four flavonoid glycosides from the pulps of Elaeagnus angustifolia and their antioxidant activities. In: Advanced Materials Research: 2013: Trans Tech Publ; 2013: 16–20.
46. El-Kersh DM, El-Sakhawy FS, Abou-Hussein DR, Sleem AA. Anabolic and androgenic effects of certain Atriplex species grown in Egypt. Egyptian J Biomed Sci. 2013;40:97–113.
47. Ali B, Musaddiq S, Iqbal S, Rehman T, Shafiq N, Hussain A. The therapeutic properties, ethno pharmacology and phytochemistry of Atriplex

species: a review. Pakistan J Biochem Biotechnol. 2021;2(1):49–64. doi: 10.52700/pjbb.v2i1.38
48. Bouzidi A, Zayen N, Saidana D, Gam W, Achour L, Mighri Z. Protein contents, total lipids and fatty acids profiles of Tunisian halophyte species: Limonium echioides, Tamarix bovena and Atriplex halimus. Tunisian J Med Plants Natural Prod. 2012;8(1):82–89.
49. Morad MY, El-Sayed H, El-Khadragy MF, Abdelsalam A, Ahmed EZ, Ibrahim AM. Metabolomic profiling, antibacterial, and molluscicidal properties of the medicinal plants Calotropis procera and Atriplex halimus: in silico molecular docking study. Plants. 2023;12(3):477. doi: 10.3390/plants12030477
50. Matloub A, El Souda S, Hamed M. Phytoconstituent of petroleum ether extract of Atriplex lindleyi Moq aerial part and its hepato-renal protection. Planta Medica. 2011;77(12):PF36. doi: 10.1055/s-0031-1282424
51. Zhang Y, Mills G, Nair M. Cyclooxygenase inhibitory and antioxidant compounds from the fruiting body of an edible mushroom. Agrocybe aegerita Phytomed. 2003;10(5):386–390. doi: 10.1078/0944-7113-00272
52. Yuan L, Zhang F, Shen M, Jia S, Xie J. Phytosterols suppress phagocytosis and inhibit inflammatory mediators via ERK pathway on LPS-triggered inflammatory responses in RAW264. 7 macrophages and the correlation with their structure. Foods. 2019;8(11):582. doi: 10.3390/foods8110582
53. Chen C, Shen J-L, Liang C-S, Sun Z-C, Jiang H-F. First discovery of beta-sitosterol as a novel antiviral agent against white spot syndrome virus. Int J Mol Sci. 2022;23(18):10448. doi: 10.3390/ijms231810448
54. Sun Y, Zhao DL, Liu ZX, Sun XH, Li Y. Beneficial effect of 20-hydroxyecdysone exerted by modulating antioxidants and inflammatory cytokine levels in collagen-induced arthritis: a model for rheumatoid arthritis. Mol Med Rep. 2017;16(5):6162–6169. doi: 10.3892/mmr.2017.7389
55. Bakrim S, Benkhaira N, Bourais I, Benali T, Lee L-H, El Omari N, Sheikh RA, Goh KW, Ming LC, Bouyahya A. Health benefits and pharmacological properties of stigmasterol. Antioxidants. 2022;11(10):1912. doi: 10.3390/antiox11101912.
56. Ziyan L, Yongmei Z, Nan Z, Ning T, Baolin L. Evaluation of the anti-inflammatory activity of luteolin in experimental animal models. Planta Med. 2007;73(03):221–226. doi: 10.1055/s-2007-967122
57. Zhang Y, Jayaprakasam B, Seeram NP, Olson LK, DeWitt D, Nair MG. Insulin secretion and cyclooxygenase enzyme inhibition by cabernet sauvignon grape skin compounds. J Agric Food Chem. 2004;52(2):228–233. doi: 10.1021/jf034616u
58. Kim D-W, Cho H-I, Kim K-M, Kim S-J, Choi JS, Kim YS, Lee S-M. Isorhamnetin-3-O-galactoside protects against CCl4-induced hepatic injury in mice. Biomol Therapeut. 2012;20(4):406. doi: 10.4062/biomolther.2012.20.4.406
59. Islam MT, Ayatollahi SA, Zihad SNK, Sifat N, Khan MR, Paul A, Salehi B, Islam T, Mubarak MS, Martins N. Phytol anti-inflammatory activity: pre-clinical assessment and possible mechanism of action elucidation. Cell Mol Biol (Noisy-le-grand) 2020;66(4):264–269. doi: 10.14715/cmb/2020.66.4.31
60. Waffo-Teguo P, Lee D, Cuendet M, Mérillon J-M, Pezzuto JM, Kinghorn AD. Two new stilbene dimer glucosides from grape (vitis v inifera) cell cultures. J Nat Prod. 2001;64(1):136–138. doi: 10.1021/np000426r
61. Cichewicz RH, Kouzi SA, Hamann MT. Dimerization of resveratrol by the grapevine pathogen Botrytis cinerea. J Nat Prod. 2000;63(1):29–33. doi: 10.1021/np990266n
62. Chansiw N, Chotinantakul K, Srichairatanakool S. Anti-inflammatory and antioxidant activities of the extracts from leaves and stems of Polygonum odoratum lour. AntiInflammatory Antiallergy Agents Med Chem. 2019;18(1):45–54. doi: 10.2174/1871523017666181109144548
63. Othman AR, Abdullah N, Ahmad S, Ismail IS, Zakaria MP. Elucidation of in-vitro anti-inflammatory bioactive compounds isolated from Jatropha curcas L plant root. BMC Complement Altern Med. 2015;15:1–10. doi: 10.1186/s12906-015-0528-4
64. Khare S, Cerda S, Wali RK, Von Lintig FC, Tretiakova M, Joseph L, Stoiber D, Cohen G, Nimmagadda K, Hart J. Ursodeoxycholic acid inhibits Ras mutations, wild-type Ras activation, and cyclooxygenase-2 expression in colon cancer. Can Res. 2003;63(13):3517–3523.

65. Bhardwaj M, Sali VK, Mani S, Vasanthi HR. Neophytadiene from Turbinaria ornata suppresses LPS-induced inflammatory response in RAW 264.7 macrophages and Sprague Dawley rats. Inflammation. 2020;43:937–950. doi: 10.1007/s10753-020-01179-z
66. Amin E, Elwekeel A, Alshariedh NF, Abdel-Bakky MS, Hassan MH. GC-MS analysis and bioactivities of the essential oil of Suaeda aegyptiaca. Separations. 2022;9(12):439. doi: 10.3390/separations9120439
67. Ma D, He J, He D. Chamazulene reverses osteoarthritic inflammation through regulation of matrix metalloproteinases (MMPs) and NF-kβ pathway in in-vitro and in-vivo models. Biosci Biotechnol Biochem. 2020;84(2):402–410. doi: 10.1080/09168451.2019.1682511
68. Hu H-J, Zhou Y, Han Z-Z, Shi Y-H, Zhang S-S, Wang Z-T, Yang L. Abietane diterpenoids from the roots of Clerodendrum trichotomum and their nitric oxide inhibitory activities. J Nat Prod. 2018;81(7):1508–1516. doi: 10.1021/acs.jnatprod.7b00814
69. Rouzer CA, Marnett LJ. Structural and chemical biology of the interaction of cyclooxygenase with substrates and non-steroidal anti-inflammatory drugs. Chem Rev. 2020;120(15):7592–7641. doi: 10.1021/acs.chemrev.0c00215.